Hydroxyapatite from biowaste for biomedical applications: obtainment, characterization and *in vitro* assays

Marla Karolyne dos Santos Horta[a*] ⓘ, *Cecília Westin*[b], *Daniel Navarro da Rocha*[c],

José Brant de Campos[d] ⓘ, *Rodrigo Fernandes Magalhães de Souza*[a] ⓘ,

Marilza Sampaio Aguilar[e] ⓘ *and Francisco José Moura*[a]

[a]*Pontifícia Universidade Católica do Rio de Janeiro, Departamento de Engenharia Química e de Materiais, 225 Marquês de São Vicente St., 22451-900, Rio de Janeiro, RJ, Brasil.*
[b]*Universidade Estadual de Campinas, Departamento de Engenharia Química, Av. Albert Einstein, 500, Zeferino Vaz, 13083-852, Campinas, SP, Brasil.*
[c]*R-Crio Criogenia S.A., Rua Cumaru 204, 13098-324, Campinas, SP Brasil.*
[d]*Universidade do Estado do Rio de Janeiro, Departamento de Engenharia Mecânica, Rua São Francisco Xavier, 524, 20550-900, Rio de Janeiro, RJ, Brasil.*
[e]*Universidade Estácio de Sá, Departamento de Química, Rua Bispo, 83, 20261-063, Rio de Janeiro, RJ, Brasil.*

The use of biogenic residues to obtain calcium phosphate compounds, mainly hydroxyapatite (HAp), is an excellent alternative to reduce costs in obtaining biomaterials. The purpose of this study was to obtain hydroxyapatite from fish bones and hen eggshells by alkaline hydrolysis and precipitation, respectively, and compare them to HAp obtained from calcium commercial source based on physical-chemical properties and *in vitro* assays. The biomaterials obtained were characterized by X-ray Diffraction (XRD), Scanning Electron Microscopy (SEM), Brunauer-Emmett-Teller (BET) method and Fourier Transform Infrared Spectroscopy (FTIR). The XRD results revealed the presence of the main characteristic peaks of single HAp phase and FTIR analysis showed various functional groups, such as PO_4^{3-}, CO_3^{-2} and OH^-, confirming the presence of HAp. SEM observations of the synthesized HAp showed a rod-like and spherical-like morphology. The cell viability and bioactivity of the materials were evaluated by rezasurin reduction and McCoy medium assays, respectively. The biomaterials obtained had no toxic effect and the sample obtained from fish bone was more bioactive when compared to the others. Therefore, the biowastes can be used as an alternative source of calcium in the synthesis of hydroxyapatite with promising properties for application in the biomedical area.

Keywords: *Hydroxyapatite, biomaterial, biowaste, eggshell, fishbone, recycling.*

1. Introduction

Every year more than 2.2 million people worldwide need a surgical procedure to repair some type of bone defect, related to critical accidents as well as trauma or degenerative diseases, such as resection of tumors, using grafts or prostheses[1]. Surgical procedures are performed using autologous bone grafts, allografts or biocompatible synthetic materials[2], which results in huge expenses with treatments for tissue diseases, and traumas[3,4].

These facts increase researches concerning the synthesis of biomaterials with better properties using economically viable processes. The great interest in hydroxyapatite (HAp) as a biomaterial is related to the mineral phase of teeth and bones, in which the HAp represents 30 to 70% in mass of hard tissue[5]. These data demonstrate the reason for its high biocompatibility and similarities with some properties of bone, including bioactivity, biodegradability and osteoconductivity[5]. Hydroxyapatite can be obtained by chemical reactions using different reagents that contain the calcium and phosphate ions, using synthetic or natural calcium sources, such as hen's eggshells[6-9], shells, corals[10,11], etc. Hydroxyapatite can also be extracted from biogenic sources, such as bovine bones, pig bones[12], fish bones and scales[13,14]. Hen's eggshells, fish bones and scales become interesting source of calcium since they are abundant and accessible, reducing the costs of raw materials and bringing environmental benefits with the use of these residues[15,16]. If these materials are improperly discarded; the organic matter present favors the growth of bacteria and fungi[17], generating undesirable consequences such as bad smell and the occurrence of disease vectors.

This study aimed to obtain hydroxyapatite from different biogenic residues, such as hen's eggshells and *Colossoma macropomum* bones, a typical freshwater fish from Brazil. The hydroxyapatite properties were compared with those obtained from a commercial calcium source aiming biomedical application. Besides that, as a result, the use of hen's eggshells and fish bones biowaste can potentially reduce the environmental issues and support sustainable environmental development.

2. Experimental

2.1. Hen's eggshell treatment

The eggshells were firstly washed with neutral soap, then boiling water to remove dirt. The eggshells were dried at 100 °C in a furnace for 5 h, then, they were calcined at 1000 °C for 2 h to remove all organic matter, and for conversion of calcium carbonate ($CaCO_3$) to calcium oxide (CaO). The hen's eggshell used came from domestic consumption.

2.2. Synthesis of hydroxyapatite samples from eggshells and commercial Ca(OH)₂

The experimental Ca/P stoichiometric ratio of 1.67 was used for all reactions carried out to obtain HAp. The synthesis was performed according to procedure described at Salma-Ancane et al.[18] with modifications.

The obtained calcium oxide (2,7g) was mixed with 50 mL of distilled water to formation of calcium hydroxide ($Ca(OH)_2$) and then mechanically stirred for 30 minutes (Stirrer Quimis-Q-235-1). The acid solution was prepared from 3,4g phosphoric acid (H_3PO_4, ISOFAR 85%) for 50mL of distilled water. The solution was added at a rate of 3.33 mL.min^{-1} [19] using a peristaltic pump, under constant stirring at room temperature. The pH was maintained in the range of 10-12[20] and corrected with ammonium hydroxide when necessary. After that, the solution was aged at room temperature for 1 h under constant stirring and then filtered and washed with distilled water to obtain a white precipitate. The precipitate was dried in a furnace at 100 °C for 5 hours. The obtained material was crushed using a mortar and pestle and then the powders were calcinated at 800 °C for 2 h in a muffle furnace. For the synthesis of HAp from the commercial calcium source, 3.7g of $Ca(OH)_2$ (ProQuimico) were used following the same procedure previously described. The obtained samples were designated as E-HAp and C-HAp for calcium source from eggshell and commercial, respectively. After the samples were calcined, the temperature used was added to the code in order to better identify them.

2.3. Extraction of hydroxyapatite from fish bone

The procedure was based on the work done by Zainol et al.[21], with modifications. The *Colossoma macropomum* bones were collected from the local fish market in Manaus city, Amazonas, Brazil. The bones were washed using tap water and the excess meat was removed manually. The bones were boiled in distilled water for 1 h to complement in the material cleaning step. Afterwards, the washed fish bones were treated with 1% (w/v) NaOH solution and heated at 90 °C for 5 h with stirring to remove all organic matter (lipids, proteins), then they were washed with distilled water for the complete removal of the NaOH solution. Thereafter, the treated bones were dried at 100 °C for 4 h in an oven, crushed with pistil and mortar and stored. The material was calcined at 800 °C and coded as FB-HAp800.

2.4. Samples characterization

The samples were characterized by X-ray diffraction in a PANalytical diffractometer, model X´Pert PRO MPD, with CuKα copper radiation, λ = 0.155418 nm with 40 kV voltage and 40 mA current. The scan was 2θ = 10°-80°, at a step size of 0.05° and acquisition rate of 2.5°min^{-1}.

The diffractograms were refined in TOPAS software-Academic program, version 4.0 using Rietveld method to determine the phase compositions and the crystallite size. Fourier Transform Infrared Spectroscopy (FTIR) analyses were performed in a Perkin Elmer Spectrum Two spectrometer. The samples were mixed with KBr, pressed to obtain pellets and analyzed. The transmission spectra were obtained in the range 4000 to 400 cm^{-1} and resolution of 4 cm^{-1}. The specific surface area of the C-HAp and E-HAp samples was determined by BET method from the N_2 gas adsorption isotherm at -196 °C (ASAP 2010 analyzer, Micromeritics Inc). The samples morphological characteristics were investigated using scanning electron microscopy (SEM), model JSM-7100F (JEOL), operating on high vacuum modes, with electron beam potential between 1 and 15kV.

2.5. In vitro assay

The powders were pressed to form 10 mm diameter pellets using 150 mg of materials in a hydraulic press (Protécni) at a pressure of 17.75 kgf.cm^{-2}. The samples were later sterilized by ethylene oxide.

2.5.1. Indirect cytotoxicity assay

The cytotoxicity test was performed for E-HAp, C-HAp and FB-HAp800 samples in human dental pulp mesenchymal stem cells (hDPSCs) obtained from a standardized sample purchased from the Lonza company (product code PT-5025, lot 0000361150) by resazurin reduction assay according to ISO 10993-5[22]. The cells were cultured in DMEM (Sigma-Aldrich), with 4500 mg.L^{-1} glucose, in the presence of 10% FBS (Gibco), and 1% Penicillin/Streptomycin (Sigma-Aldrich) at 37 °C in a humidified atmosphere of 5% CO_2 incubator.

The samples extracts were obtained by incubating 0.1 g of dry material per mL of culture medium for 24h (group 1) and 48 h (group 2) in the incubator at 37 °C, 5% CO_2 atmosphere. The cells were seeded at a density of 4×10^4 cells/well in a 96-well plate and cultured for 24 h to allow cell adhesion. After 24 h, the cells were incubated with 100 μL of the extracts for more 24 h (37 °C, 5% CO_2, humidified atmosphere). For positive viability reference (positive control), it was used supplemented culture medium, while 50% (v/v) of dimethyl sulfoxide (DMSO) with supplemented culture medium was used as negative reference (negative control). All experiments were performed in triplicate. After the incubation period, the extracts were replaced for 200 μL of resazurin solution (Sigma-Aldrich) (0.5 mg.L^{-1} resazurin in PBS, diluted in standard culture medium at 50% v/v)[23]. The cells were again incubated for 4 h. After incubation, 100 μL aliquots were collected and transferred to another 96-well plate, where fluorescence analysis was performed on a spectrophotometer with a microplate reader (Biotek Synergy HT) at wavelengths of 530 nm excitation and 590 nm emission. The percentage of viable cells was calculated from the average values of absorbance for each sample in relation to the positive control defined as 100%.

Cell viability results were subjected to analysis of variance (ANOVA) and Tukey's test using PAST software. Results with P values < 0.05 are considered statistically significant. All results are expressed as mean values with standard deviations.

2.5.2. Bioactivity assay

For bioactivity assessment, the E-HAp, C-HAp and FB-HAp800 pellets were immersed in 16 mL McCoy`s 5A[23-25] (Vitrocell) medium in Falcon tubes with in aseptic conditions using laminar flow hood. The samples were maintained at 37 °C under 5% CO_2 atmosphere, in an incubator (PANASONIC, COM-19AIC-PA model) for 3 and 7 days[25-28]. The solution was changed every 3 days. The pellets were analyzed by SEM to observe the surface characteristics of the samples after the immersion period.

3. Results and Discussion

3.1. Samples characterization

The N_2 adsorption/desorption isotherms for E-HAp and C-HAp particles obtained from eggshell and calcium source commercial, respectively, are shown in Figure 1.

The isotherms have hysteresis loops and can be classified as type IV[29,30]. The isotherms of these two samples were slightly different. For the E-HAp sample, the isotherm exhibited a slightly steeper slope in relation to the C-HAp sample, which may be related to a narrow pore size distribution. The slope of the curve in the capillary condensation region reflects the pore size distribution, the softer the slope, the greater the pore size heterogeneity in the sample[31].

The pore diameter, pore volume and specific surface area of the samples measured using BET are summarized in Table 1.

The E-HAp sample with larger pore size of 31.75 nm is classified as mesoporous and the C-HAp sample is classified as microporous according to IUPAC. The E-HAp and C-HAp samples showed specific surface values of 85.8 and 133.7 $m^2.g^{-1}$, respectively, and the pore volume values of about 0.55$cm^3.g^{-1}$ for both samples. The results obtained are similar to those reported by Salma-Ancane et al.[18] when comparing HAp from a commercial and natural calcium source using a slower addition rate and aging time higher than those used in this work. As the sources of calcium are different, biogenic and commercial, they may present particles with different sizes, possibly influencing the characteristics of synthesized HAp.

The pore size has direct implications for their functionality for biomedical applications. The presence of pores in materials combined with their biodegradation can improve cell access to different regions during tissue regeneration. The pore network structures facilitate transport of nutrients and metabolites, guiding and promoting the tissue formation[32]. The specific surface area results of the synthesized HAp are in the range of values reported in the literature for natural bones, such as femur and dentin, ranging from 8 to 100 $m^2.g^{-1}$[33-34]. The pore diameter values qualify the E-HAp samples to be used in controlled drug delivery systems. The pore diameter has a strong influence on the release rate of the molecules. The specific surface area, size and volume pores are parameters that can affect the kinetics of adsorption and release of drugs.

The crystal structure and phase content of the different samples were identified using XRD patterns. Figure 2

shows the diffractograms of the "green" (as-synthesised) and calcinated samples at 800 °C. The XRD patterns showed all samples having an apatite structure according to ICSD 34457 correspond to hydroxyapatite. The diffractograms profile of the uncalcined samples have wide and flattened peaks, mainly the sample FB-HAp. The wider the peaks, the organization of the occupation is more imperfect. The smaller the width of the peaks, the closer to the ideal condition the atomic occupation is.
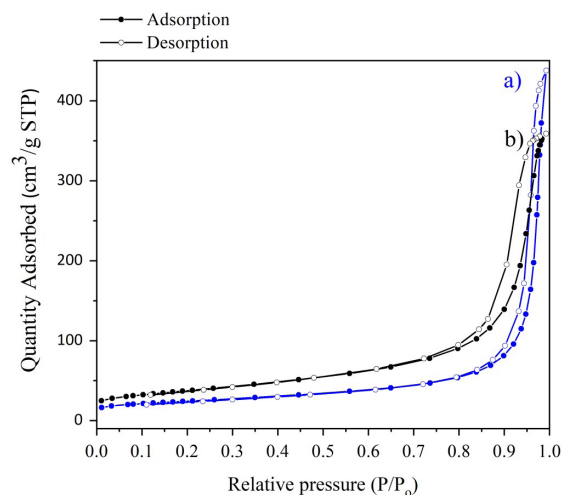
Figure 1. Adsorption–desorption isotherms of N_2 of (a) E- HAp and (b) C-HAp samples.
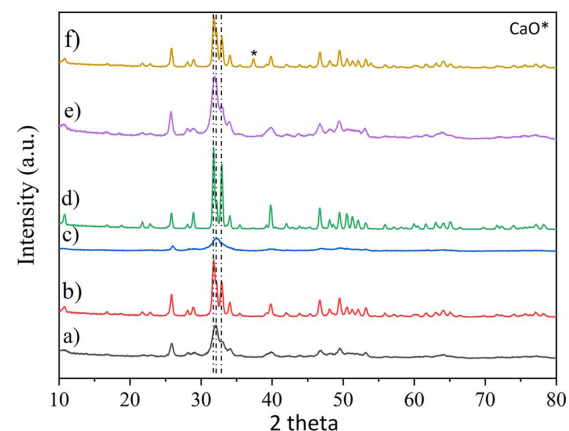
Figure 2. X-ray diffraction patterns of the samples before and after calcination at 800 °C. (a) E-HAp, (b) E-HAp800, (c) FB-HAp, (d) FB-HAp800, (e) C-HAp and (f) C-HAp800.

Table 1. BET results, specific surface area, pore diameter and pore volume for the synthesized samples.

| Samples	S_{BET} $(m^2.g^{-1})$	Pore diameter (nm)	Pore volume $(cm^3.g^{-1})$
E-HAp	85.8	31.75	0.57
C-HAp	133.7	17.51	0.54

The diffractograms of the samples E-HAp, E-HAp800, C-HAp, C-HAp800, FB-HAp, and FB-HAp800 were refined by the Rietveld method, obtaining the quantification of the phases and the results of crystallite size are shown in the Table 2.

The XRD patterns of all HAp samples after treatment at 800 °C (Figure 2) showed the characteristic peaks of HAp with better definition of the three main planes (211), (112) and (300). The heat treatment promotes a phase change in the hydroxyapatite structure, from monoclinic to hexagonal. According to Corno et al.[35] and Zahn and Hochrein[36] this transformation is favoured from 200 °C. As can be seen in Figure 2, as the temperature increases, the peaks become narrower and more defined. In the C-HAp800 sample was identified a peak at 2θ equal to 37.346°, referring to CaO. The E-HAp800 and FB-HAp800 samples presented only the hydroxyapatite phase, which were stable for the temperatures used in the heat treatment. In the sample C-HAp800, through refinement by the Rietveld method, 2.3% CaO was identified, indicating lower thermal stability of the material in relation to the others. It can be argued that the aging time was not enough for the stability of the hydroxyapatite obtained from commercial calcium source. The C-HAp, FB-HAp and E-HAp samples have a crystallite size of 16.64, 9.18 and 13.82 nm, respectively. The samples C-HAp800, FB-HAp800 and E-HAp800 have crystallite size of 37.84, 58.62 and 47.23 nm, respectively. These results obtained are consistent with those reported in the literature[37,38].

FTIR was also used to identify the functional groups present in the HAp powder obtained from different sources and results are given in Figure 3.

Table 2 Crystallite size values of the samples obtained.

Samples	Crystallite size (nm)
C-HAp	16.64
C-HAp800	37.84
FB-HAp	9.18
FB-HAp800	58.62
E-HAp	13.82
E-HAp800	47.23
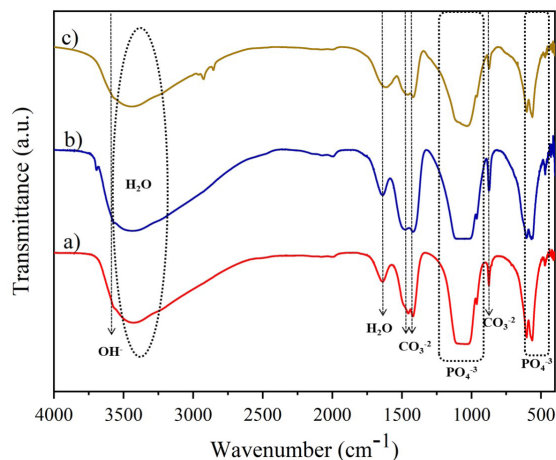
Figure 3. FTIR spectra of (a) E-HAP, (b) C-HAp and (c) FB-HAp samples.

The FTIR results show similar spectra for the three samples at around 3000–3700 cm^{-1} which are characteristic of the OH- stretching of H_2O. A second region referring to the (OH$^-$) of H_2O band can be seen in 1641 cm^{-1}. The regions at 1120–1028 cm^{-1} and 470 cm^{-1} contain the peaks due to the PO_4^{3-} stretching mode. The bands at 958, 563 and 603 cm^{-1} are the characteristic peaks of PO_4^{3-} bending mode. The small bands spotted 3567–3574 cm^{-1} were due to stretching vibration of OH$^-$ groups. These bands were observed only in samples E-HAp and C-HAp. The bands at 872, 1415 e 1455 cm^{-1} were due to the presence of carbonate. These peaks are associated with bending in B type carbonate hydroxyapatite due to the substitution of PO_4^{3-} by CO_3^{-2} [19,39-42]. The presence of carbonated groups is common in biological HAp, with the highest concentration, from 4 to 6% of ions[43], making the samples analogous to biological apatites. The carbonate substitution is particularly important for the mineral phase of bone and has proven to have osteointegration, good biocompatibility and earlier bioresorption compared to normal HAp[38,44-46]. The bands obtained for the respective phosphates and hydroxyl groups of HAp are in accordance with the data reported in the literature[18,38,47-51]. The FTIR spectrum of the FB-HAp sample showed amide peaks only at 2923 and 2853 cm^{-1} in low intensity. Based on this last result, it can be deduced that the organic part was removed almost entirely from the raw fish bones making it possible to obtain HAp.

The SEM micrographs of the HAp powder derived from different sources are shown in Figure 4. Scanning electron microscopy was used to analyze the morphology and surface of the samples. The E-HAp and C-HAp samples have rod-like morphology. This morphology has been reported by different authors[19,38,52,53]. From the micrographs it can be assumed that they have a similar size. The FB-HAp sample has a very formation of agglomerated nanoparticles with irregular shapes, whereas the FB-HAp800 sample is composed of particles with a more defined morphology, presenting a faceted surface and a larger size in relation to the others. The morphology was reported by Zainol et al.[21], for HAp obtained from tilapia fish scales. And all the samples have smooth surface, except for the sample FB-HAp, which has a very rough surface.

3.2. In vitro assays

3.2.1. Indirect cytotoxicity

The indirect contact assay was performed using extracts obtained for 24h (group 1) and 48h (group 2) of E-HAp, C-HAp and FB-HAp800 samples. The extracts that were tested to dental pulp stem cells by resazurin reduction assay evaluated the metabolic function and cellular health. In Figure 5 are presented the results after 24h of incubation.

The cell viability for the extracts obtained for the 24h period was 93.3 ±5.5%, 105.7 ±2.6% and 96.7 ±2.7% for the samples E-HAp, C-HAp, and FB-HAp800, respectively. And for the extracts obtained for the 48h period, the viability was 87.2 ±2.3%, 98.9 ±2.2% and 104.6 ±0.4% following the same order as the previous one. The values of 105.7% and 104.6% for the E-HAp and FB-HAp samples is an indication of increased cell activity resulting from cell growth since cell viability was greater than 100% of the positive control.
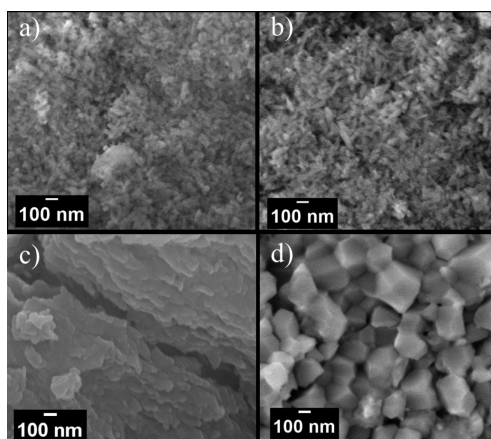
Figure 4. Scanning electron microscopy images for (a) E-HAp, (b) C-HAp, (c) FB-HAp and (d) FB-HAp800 samples.

According to ISO 10993-5[22], the reduction of cell viability by more than 30% is considered a cytotoxic effect, thus, no cytotoxicity to dental pulp stem cells was observed for any of the samples because the percentages of viable cells were above 87%. The results are not statistically significant (p>0.05).

In the work carried out by Ingole et al.[54] superior cell viability was also observed for the synthetic HAp sample compared to that derived from chicken eggshells. However, research with different biogenic sources such as bovine bone and shells were superior to synthetic HAp from commercial sources[55,56], result that can be observed for the sample FB-HAp800 in relation to C-HAp sample. Such results show that the calcium phosphate compounds obtained from natural sources present similar and/or superior results to those presented by samples synthesized from commercial calcium sources.

The E-HAP and C-HAp samples showed lower cell viability for the extracts obtained in 48h and it can be attributed to the ions release concentration combined with the particle size were responsible for the difference in relation to the extract obtained in 24h. The sample FB-HAp800 showed an inverse behavior, presenting cell growth for the extract obtained in 48h. This sample presented a particle size higher than the others as verified in SEM, which reinforce the influence of particle size on cell viability. Many studies report the relationship of particle size in the material cytotoxic responses, since the smaller the particle, the greater the tendency to enter subcellular organelles and provide greater cytotoxicity. Besides, there is a relationship with the concentration that can directly affect cell activity[57-59]. The cellular response is due to a group of factors that will act together to reach a result. Limits on size, morphology, and concentration concerning the application of the material must be identified.

3.2.2. Bioactivity

Figure 6 shows the bioactivity assay results for the samples analysed. The McCoy solution was used to simulate the physiological conditions with typical concentrations of ions in the human body (under controlled conditions of pressure, temperature and atmosphere) to evaluate characteristics such as dissolution, morphology and the formation of the bone like apatite layer on the surface of the samples.
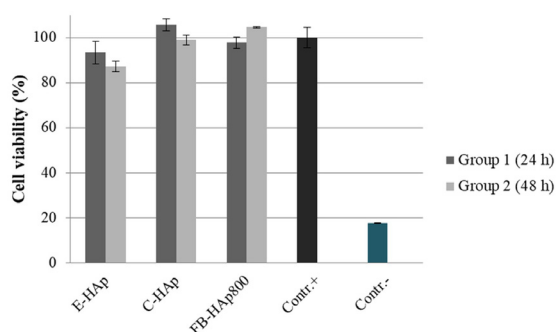

Figure 5. Indirect cytotoxicity of the samples to dental pulp stem cells for a 24h incubation period. Cell culture with standard supplemented culture medium was used as positive control (Contr.+) and with 50% (v/v) DMSO in PBS as negative control (Contr.-) of toxicity.

The McCoy medium has been used in preference to the SBF (Simulated Body Fluid) due to its composition is much more similar to body fluids, which has the presence of macromolecules and proteins, in equilibrium at CO_2 partial pressure[60].

The E-HAp and C-HAp samples showed the formation of grooves after 3 and 7 days of immersion in McCoy medium (indicated by white arrows). Nevertheless, the deposition of the *bone like apatite* layer was not verified. The formation of grooves is due to the release of material into the environment. Greater resorption of these samples was already expected, since they have relatively low crystallinity and small crystallite size, as observed in the XRD results.

The FB-HAp800 sample presented after 7 days of immersion, which can be considered the beginning of the formation of the apatite layer through the formation of a filamentous structure on the particles. A similar result was reported by Horta et al.[14] for 3 days of immersion in McCoy medium for hydroxyapatite extracted from Osteoglossum bicirrhosum fish scales. It can be stated that the time used in the study was not enough for the growth of the layer for the C-Hap and E-HAp samples. The deposition of the bone like apatite layer is related to numerous factors such as method of preparing the material, surface characteristics, among others, which makes the material to have different responses for the incubation periods used.
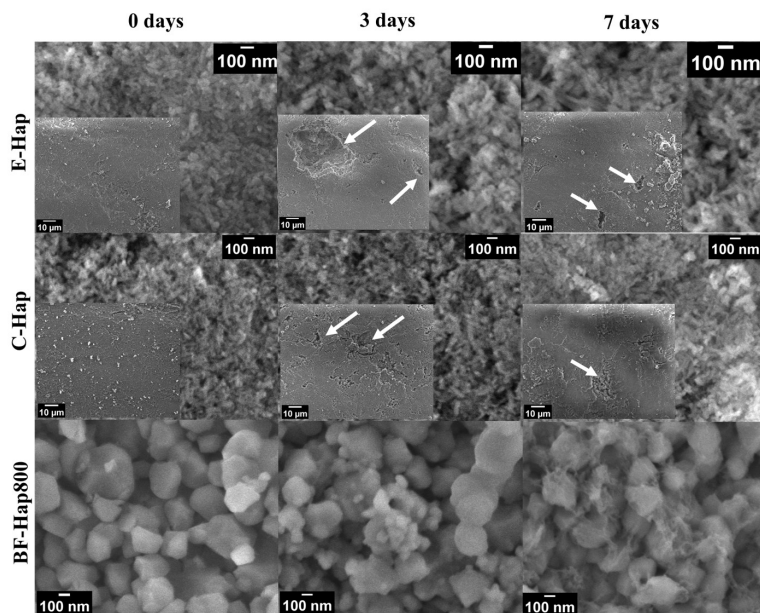
Figure 6. Comparison of samples for different periods of immersion in McCoy solution. The arrows indicate the grooves formed due to the dissolution process.

Asadollahzadeh et al.[27] performed bioactivity tests in SBF medium and obtained different responses to the same material for the same incubation period. The authors studied HAp obtained from heat-treated tuna bone at 600 ° and 900 °C. The sample treated at 600 °C only showed the formation of the apatite layer after 14 days, while the sample treated at 900 °C showed the formation of the layer after 7 days of soaking in SBF.

The literature reports research with different times of immersion, like 3, 7, 14, 21 and 28 days[25,28,61-64]. For the incubation period used in this work, HAp derived from fish bone showed a faster bioactivity response compared to samples from eggshell and commercial calcium source in McCoy medium reinforcing that the response time for the bioactivity of the material depends on numerous factors, among them, the methods of obtaining the material.

4. Conclusions

HAp biomaterials were successfully obtained from natural source like fish bones and through chemical precipitation method using hen's eggshell. This work reinforces the use of bio-sources to obtain hydroxyapatite to application as biomaterial, in order to obtain materials with low production costs and relatively simple techniques. This work is the first record in the literature regarding the use of the *Colossoma macropomum* fish bones. The studied in McCoy medium confirmed that the FB-HAp800 had a superior ability to induce apatite formation as observed in the results obtained from SEM showing the growth of the apatite layer starting at 7 days. The in vitro cell culture studies confirmed the non-cytotoxic of the samples because the percentages of viable cells were above 87%. These preliminary results suggest that the synthesized HAp from hen's eggshells and extracted from fish bones, materials considered waste, has potential application in tissue engineering.

Therefore, the present study provides evidence that supports the valorization of biowastes as feedstock to produce economically feasible of HAp.

References

1. Javaid MA, Kaartinen MT. Mesenchymal stem cell-based bone tissue engineering. Int Dent J Stud Res. 2013;1:24-35.
2. Neovius E, Engstrand T. Craniofacial reconstruction with bone and biomaterials: review over the last 11 years. J Plast Reconstr Aesthet Surg. 2010;63(10):1615-23.
3. Zethraeus N, Borgstrom F, Strom O, Kanis JA, Jonsson B. Cost-effectiveness of the treatment and prevention of osteoporosis - a review of the literature and a reference model. Osteoporos Int. 2007;18(1):9-23.
4. Zhou Y, Zhao Y, Wang L, Xu L, Zhai M, Wei S. Radiation synthesis and characterization of nanosilver/gelatin/carboxymethyl chitosan hydrogel. Radiat Phys Chem. 2012;81(5):553-60.
5. Dorozhkin SV. Calcium orthophosphates as bioceramics: state of the art. J Funct Biomater. 2010;1(1):22-107.
6. Horta M, Aguilar M, Moura F, Campos J, Ramos V, Quizunda A. Synthesis and characterization of green nanohydroxyapatite from hen eggshell by precipitation method. Mater Today Proc. 2019;14:716-21.

7. Aguilar MS, Quizunda AC, Moura FJ, Campos JB, Machado MVF, Horta MKSH et al. Viabilidade do uso de cascas de ovos na síntese da hidroxiapatita utilizando o método sol-gel. In: Abdala MRWS, editor. A aplicação do conhecimento científico nas engenharias. Ponta Grossa: Atena Editora; 2019. p. 54-62. https://orcid.org/10.22533/at.ed.4491904046.

8. Horta MKDS, Moura FJ, Aguilar MS, Westin CB, Campos JBD, Peripolli SB et al. Nanostructured hydroxyapatite from Hen´s eggshells using sucrose as a template. Mater Res. 2020;23(6):e20200266.

9. Núñez D, Elgueta E, Varaprasad K, Oyarzún P. Hydroxyapatite nanocrystals synthesized from calcium rich bio-wastes. Mater Lett. 2018;230:64-8.

10. Rujitanapanich S, Kumpapan P, Wanjanoi P. Synthesis of hydroxyapatite from oyster shell via precipitation. Energy Procedia. 2014;56:112-7.

11. Wu SC, Hsu HC, Hsu SK, Tseng CP, Ho WF. Preparation and characterization of hydroxyapatite synthesized from oyster shell powders. Adv Powder Technol. 2017;28(4):1154-8.

12. Ramesh S, Loo ZZ, Tan CY, Chew WK, Ching YC, Tarlochan F et al. Characterization of biogenic hydroxyapatite derived from animal bones for biomedical applications. Ceram Int. 2018;44(9):10525-30.

13. Shi P, Liu M, Fan F, Yu C, Lu W, Du M. Characterization of natural hydroxyapatite originated from fish bone and its biocompatibility with osteoblasts. Mater Sci Eng C. 2018;90:706-12.

14. Horta MKDS, Moura FJ, Aguilar MS, Westin CB, Rocha DN, Campos JB. In vitro evaluation of natural hydroxyapatite from Osteoglossum bicirrhosum fish scales for biomedical application. Int J Appl Ceram Technol. 2021;18(6):1930-7.

15. Sadat-Shojai M, Khorasani MT, Dinpanah-Khoshdargi E, Jamshidi A. Synthesis methods for nanosized hydroxyapatite with diverse structures. Acta Biomater. 2013;9(8):7591-621.

16. Murakami FS, Rodrigues PO, Campos CMTD, Silva MAS. Physicochemical study of CaCO3 from egg shells. Food Sci Technol. 2007;27:658-62.

17. Rivera EM, Araiza M, Brostow W, Castano VM, Díaz-Estrada JR, Hernández R et al. Synthesis of hydroxyapatite from eggshells. Mater Lett. 1999;41(3):128-34.

18. Salma-Ancane K, Stipniece L, Irbe Z. Effect of biogenic and synthetic starting materials on the structure of hydroxyapatite bioceramics. Ceram Int. 2016;42(8):9504-10.

19. Ibrahim AR, Zhou Y, Li X, Chen L, Hong Y, Su Y et al. Synthesis of rod-like hydroxyapatite with high surface area and pore volume from eggshells for effective adsorption of aqueous Pb (II). Mater Res Bull. 2015;62:132-41.

20. Lynn AK, Bonfield W. A novel method for the simultaneous, titrant-free control of pH and calcium phosphate mass yield. Acc Chem Res. 2005;38(3):202-7.

21. Zainol I, Adenan NH, Rahim NA, Jaafar CA. Extraction of natural hydroxyapatite from tilapia fish scales using alkaline treatment. Mater Today Proc. 2019;16:1942-8.

22. ISO: International Organization for Standardization. ISO 10993-10995: biological evaluation of medical. Geneva: International Organization for Standardization; 2009.

23. Souza RFB, Souza FCB, Rodrigues C, Drouin B, Popat KC, Mantovani D et al. Mechanically-enhanced polysaccharide-based scaffolds for tissue engineering of soft tissues. Mater Sci Eng C. 2019;94:364-75.

24. Lee J, Leng Y, Chow KL, Ren F, Ge X, Wang K et al. Cell culture medium as an alternative to conventional simulated body fluid. Acta Biomater. 2011;7(6):2615-22.

25. Rocha DN, Cruz LRO, Campos JB, Santos JL, Marçal RLSB, Mijares DQ et al. Bioactivity of strontium-monetite coatings for biomedical applications. Ceram Int. 2019;45(6):7568-79.

26. Fonseca FM, Costa AM, Campos JB, Marçal RLSB, Rocha DN. Bioactivity assessment of Ag-HA. Biomater Med Appl. 2017;1(2):2-5.

27. Asadollahzadeh M, Rabiee SM, Salimi-Kenari H. In vitro apatite formation of calcium phosphate composite synthesized from fish bone. Int J Appl Ceram Technol. 2019;16(5):1969-78.

28. Bonadio TG, Freitas VF, Tominaga TT, Miyahara RY, Rosso JM, Cótica LF et al. Polyvinylidene fluoride/hydroxyapatite/β-tricalcium phosphate multifunctional biocomposite: potentialities for bone tissue engineering. Curr Appl Phys. 2017;17(5):767-73.

29. Wang H, Zhai L, Li Y, Shi T. Preparation of irregular mesoporous hydroxyapatite. Mater Res Bull. 2008;43(6):1607-14.

30. Ng S, Guo J, Ma J, Loo SCJ. Synthesis of high surface area mesostructured calcium phosphate particles. Acta Biomater. 2010;6(9):3772-81.

31. Kruk M, Jaroniec M, Sayari A. Relations between pore structure parameters and their implications for characterization of MCM-41 using gas adsorption and X-ray diffraction. Chem Mater. 1999;11(2):492-500.

32. Loh QL, Choong C. Three-dimensional scaffolds for tissue engineering applications: role of porosity and pore size. Tissue Eng Part B Rev. 2013;19(6):485-502.

33. Joschek S, Nies B, Krotz R, Göpferich A. Chemical and physicochemical characterization of porous hydroxyapatite ceramics made of natural bone. Biomaterials. 2000;21(16):1645-58.

34. Misra DN, Bowen RL, Mattamal GJ. Surface area of dental enamel, bone, and hydroxyapatite: chemisorption from solution. Calcif Tissue Res. 1978;26:139-42.

35. Corno M, Rimola A, Bolis V, Ugliengo P. Hydroxyapatite as a key biomaterial: quantum-mechanical simulation of its surfaces in interaction with biomolecules. Phys Chem Chem Phys. 2010;12(24):6309-29.

36. Zahn D, Hochrein O. A molecular dynamics simulation study of (OH−) Schottky defects in hydroxyapatite. Z Anorg Allg Chem. 2005;631(6-7):1134-8.

37. Goloshchapov DL, Kashkarov VM, Rumyantseva NA, Seredin PV, Lenshin AS, Agapov BL et al. Synthesis of nanocrystalline hydroxyapatite by precipitation using hen's eggshell. Ceram Int. 2013;39(4):4539-49.

38. Sanosh KP, Chu MC, Balakrishnan A, Lee YJ, Kim TN, Cho SJ. Synthesis of nano hydroxyapatite powder that simulate teeth particle morphology and composition. Curr Appl Phys. 2009;9(6):1459-62.

39. Berzina-Cimdina L, Borodajenko N. Research of calcium phosphates using Fourier transform infrared spectroscopy. In: Theophanides T, editor. Infrared spectroscopy: materials science, engineering and technology. Rijeka: InTech; 2012. p. 251-63.

40. Paul S, Pal A, Choudhury AR, Bodhak S, Balla VK, Sinha A et al. Effect of trace elements on the sintering effect of fish scale derived hydroxyapatite and its bioactivity. Ceram Int. 2017;43(17):15678-84.

41. Sathiskumar S, Vanaraj S, Sabarinathan D, Bharath S, Sivarasan G, Arulmani S et al. Green synthesis of biocompatible nanostructured hydroxyapatite from Cirrhinus mrigala fish scale–a biowaste to biomaterial. Ceram Int. 2019;45(6):7804-10.

42. Wu SC, Hsu HC, Hsu SK, Chang YC, Ho WF. Effects of heat treatment on the synthesis of hydroxyapatite from eggshell powders. Ceram Int. 2015;41(9):10718-24.

43. Dorozhkin SV. Calcium orthophosphates in nature, biology and medicine. Materials. 2009;2(2):399-498.

44. Porter A, Patel N, Brooks R, Best S, Rushton N, Bonfield W. Effect of carbonate substitution on the ultrastructural characteristics of hydroxyapatite implants. J Mater Sci Mater Med. 2005;16:899-907.

45. Landi E, Tampieri A, Mattioli-Belmonte M, Celotti G, Sandri M, Gigante A et al. Biomimetic Mg-and Mg, CO3-substituted hydroxyapatites: synthesis characterization and in vitro behaviour. J Eur Ceram Soc. 2006;26(13):2593-601.

46. Boanini E, Gazzano M, Bigi A. Ionic substitutions in calcium phosphates synthesized at low temperature. Acta Biomater. 2010;6(6):1882-94.

47. Shu C, Xianzhu Y, Zhangyin X, Guohua X, Hong L, Kangde Y. Synthesis and sintering of nanocrystalline hydroxyapatite powders by gelatin-based precipitation :method. Ceram Int. 2007;33(2):193-6.

48. Brundavanam RK, Jiang ZT, Chapman P, Le XT, Mondinos N, Fawcett D et al. Effect of dilute gelatine on the ultrasonic thermally assisted synthesis of nano hydroxyapatite. Ultrason Sonochem. 2011;18(3):697-703.

49. Othmani M, Aissa A, Grelard A, Das RK, Oda R, Debbabi M. Synthesis and characterization of hydroxyapatite-based nanocomposites by the functionalization of hydroxyapatite nanoparticles with phosphonic acids. Colloids Surf A Physicochem Eng Asp. 2016;508:336-44.

50. Higuita LP, Vargas AF, Gil MJ, Giraldo LF. Synthesis and characterization of nanocomposite based on hydroxyapatite and monetite. Mater Lett. 2016;175:169-72.

51. Ramesh S, Natasha AN, Tan CY, Bang LT, Ching CY, Chandran H. Direct conversion of eggshell to hydroxyapatite ceramic by a sintering method. Ceram Int. 2016;42(6):7824-9.

52. Zuo G, Wei X, Sun H, Liu S, Zong P, Zeng X et al. Morphology controlled synthesis of nano-hydroxyapatite using polyethylene glycol as a template. J Alloys Compd. 2017;692:693-7.

53. Molino G, Palmieri MC, Montalbano G, Fiorilli S, Vitale-Brovarone C. Biomimetic and mesoporous nano-hydroxyapatite for bone tissue application: a short review. Biomed Mater. 2020;15(2):022001.

54. Ingole VH, Hussein KH, Kashale AA, Ghule K, Vuherer T, Kokol V et al. Ultrasound-assisted green economic synthesis of hydroxyapatite nanoparticles using eggshell biowaste and study of mechanical and biological properties for orthopedic applications. J Biomed Mater Res A. 2017;105(11):2935-47.

55. Sun RX, Lv Y, Niu YR, Zhao XH, Cao DS, Tang J et al. Physicochemical and biological properties of bovine-derived porous hydroxyapatite/collagen composite and its hydroxyapatite powders. Ceram Int. 2017;43(18):16792-8.

56. Miculescu F, Mocanu AC, Stan GE, Miculescu M, Maidaniuc A, Cîmpean A et al. Influence of the modulated two-step synthesis of biogenic hydroxyapatite on biomimetic products' surface. Appl Surf Sci. 2018;438:147-57.

57. Yang X, Li Y, Liu X, Zhang R, Feng Q. In vitro uptake of hydroxyapatite nanoparticles and their effect on osteogenic differentiation of human mesenchymal stem cells. Stem Cells Int. 2018;2018:2036176.

58. Zhao X, Ng S, Heng BC, Guo J, Ma L, Tan TTY et al. Cytotoxicity of hydroxyapatite nanoparticles is shape and cell dependent. Arch Toxicol. 2013;87:1037-52.

59. Rao CY, Sun XY, Ouyang JM. Effects of physical properties of nano-sized hydroxyapatite crystals on cellular toxicity in renal epithelial cells. Mater Sci Eng C. 2019;103:109807.

60. Bohner M, Lemaitre J. Can bioactivity be tested in vitro with SBF solution? Biomaterials. 2009;30(12):2175-9.

61. Fahami A, Beall GW, Betancourt T. Synthesis, bioactivity and zeta potential investigations of chlorine and fluorine substituted hydroxyapatite. Mater Sci Eng C. 2016;59:78-85.

62. Kumar GS, Govindan R, Girija EK. In situ synthesis, characterization and in vitro studies of ciprofloxacin loaded hydroxyapatite nanoparticles for the treatment of osteomyelitis. J Mater Chem B Mater Biol Med. 2014;2(31):5052-60.

63. Zima A. Hydroxyapatite-chitosan based bioactive hybrid biomaterials with improved mechanical strength. Spectrochim Acta A Mol Biomol Spectrosc. 2018;193:175-84.

64. Deb P, Deoghare AB. Effect of acid, alkali and alkali–acid treatment on physicochemical and bioactive properties of hydroxyapatite derived from catla catla fish scales. Arab J Sci Eng. 2019;44(9):7479-90.